

Cancer Chemotherapy in Early Life Significantly Alters the Maturation of Pain Processing

G. J. Hathway,^{b,c,*} Emily Murphy,^a Joseph Lloyd,^{b,c} Charles Greenspon^{b,c} and R. P. Hulse^{a,b,c,*}

^a Cancer Biology, School of Medicine, University of Nottingham, Nottingham NG7 2UH, United Kingdom

^b School of Life Sciences, University of Nottingham, Nottingham NG7 2UH, United Kingdom

^c School of Science and Technology, Nottingham Trent University, Clifton Lane, Nottingham NG11 8NS, United Kingdom

Abstract—Advances in pediatric cancer treatment have led to a ten year survival rate greater than 75%. Platinum-based chemotherapies (e.g. cisplatin) induce peripheral sensory neuropathy in adult and pediatric cancer patients. The period from birth through to adulthood represents a period of maturation within nociceptive systems. Here we investigated how cisplatin impacts upon postnatal maturation of nociceptive systems. Neonatal Wistar rats (Postnatal day (P) 7) were injected (i.p.) daily with either vehicle (PBS) or cisplatin (1mg/kg) for five consecutive days. Neither group developed mechanical or thermal hypersensitivity immediately during or after treatment. At P22 the cisplatin group developed mechanical ($P < 0.05$) and thermal ($P < 0.0001$) hypersensitivity versus vehicle group. Total DRG or dorsal horn neuronal number did not differ at P45, however there was an increase in intraepidermal nerve fiber density in cisplatin-treated animals at this age. The percentage of IB₄+ve, CGRP+ve and NF200+ve DRG neurons was not different between groups at P45. There was an increase in TrkA+ve DRG neurons in the cisplatin group at P45, in addition to increased TrkA, NF200 and vGLUT2 immunoreactivity in the lumbar dorsal horn versus controls. These data highlight the impact pediatric cancer chemotherapy has upon the maturation of pain pathways and later life pain experience.

This article is part of a Special Issue entitled: SI: Pain Circuits. Crown Copyright © 2017 Published by Elsevier Ltd on behalf of IBRO. This is an open access article under the CC BY license (<http://creativecommons.org/licenses/by/4.0/>).

Key words: cisplatin, neuropathy, pain, hyperalgesia, development, postnatal.

INTRODUCTION

Platinum-based chemotherapies (e.g. oxaliplatin, cisplatin) are front line cancer treatments (van As et al., 2012). However, these cytotoxic drugs not only target cancerous cells but also other non-cancerous cell types and thus produce considerable side-effects. Up to 95% of adult patients suffer from sensory complications (e.g. pain, numbness) during or following chemotherapy, which typically affect the extremities (hands and feet) (Paice, 2011; Giles et al., 2007). Consequently chemotherapy-induced sensory neuropathies (CIPN) can impede success of treatment and in some cases lead to treatment being terminated (Park et al., 2013). Many adult-patients suffer CIPN after initial cisplatin exposure (McWhinney et al., 2009), which can persist for many months following cessation of treatment (Seretny et al., 2014). Cisplatin-induced CIPN has been investigated

extensively in rodent models (Joseph and Levine, 2009; Uhelski et al., 2015) with translatable hallmarks of sensory neuropathy presented such as sensory neuron degeneration (intraepidermal sensory nerve fiber (IENF) innervation loss and axonal degeneration) (Ta et al., 2006; Mao-Ying et al., 2014) and sensory neuron hyperexcitability (Joseph and Levine, 2009; Uhelski et al., 2015).

Despite the significant implications for adult cancer survivors, understanding the impact of chemotherapy-induced sensory neurotoxicity upon childhood cancer survivors has not been extensively investigated. Against a background of increased cancer patient survival rates in the general population, improvements in treating pediatric cancer has resulted in survival rates of ~75% surviving longer than 5–10 years (Smith et al., 2010; Ward et al., 2014). Pediatric cancer treatments are similarly invasive to that in adults, with highly cytotoxic agents administered and surgical interventions often required. Evidence exists to show that chemotherapy treatment early in life leads to a significant decline in quality of life in adult childhood cancer survivors. Typically many patients complain of fatigue, anxiety and depression (Clanton et al., 2011; Kunin-Batson et al., 2016) as well

*Corresponding authors. Address: School of Life Sciences, University of Nottingham, Queen's Medical Centre, West Block, D Floor, Nottingham NG7 2UH, United Kingdom (G.J. Hathway). School of Science and Technology, Nottingham Trent University, Clifton Lane, Nottingham NG11 8NS, United Kingdom (R.P. Hulse).
 E-mail addresses: gareth.hathway@nottingham.ac.uk (G. J. Hathway), Richard.Hulse@NTU.ac.uk (R. P. Hulse).

as impairment of the auditory system that significantly effects social interactions and cognitive development (Grewal et al., 2010). However, exposure to chemotherapy at a young age leads to pain (Lu et al., 2011), especially in the extremities (hands, arms) Lu et al., 2011; Gilchrist et al., 2014 and alterations in sensory function (Ness et al., 2013). This pain manifests itself in adulthood many years after diagnosis and discontinuation of treatment (Ness et al., 2013; Khan et al., 2014; Phillips et al., 2015). Cisplatin is a commonly utilized chemotherapeutic agent used in pediatric oncology, for example in treating hepatoblastoma (Zsiros et al., 2010; Zsiros et al., 2013) and studies investigating neuropathy in survivors demonstrate that cisplatin treatment early in life leads to the develop of pain in adulthood in these patients (Gilchrist and Tanner, 2013; Gilchrist et al., 2014). However, there has currently been no investigation into the mechanistic avenues by which cisplatin induces pain in childhood cancer survivors.

Nociceptive pathways are not fully developed at birth and maturation of the sensory nervous system during early life is greatly manipulated by disease and injury (Fitzgerald, 2005). During infancy the peripheral nervous system is still developing. The central terminals of primary afferent sensory neurons are still to be ‘hard wired’ and physiological properties of dorsal horn networks that are activated by these afferents are also immature. Nerve injury early in life has been shown to result in a pronounced hyperalgesia that emerges in adulthood (Vega-Avelaira et al., 2012; McKelvey et al., 2015). This study was designed to determine whether cisplatin treatment early in life leads to an alteration in pain perception in adulthood. In Sprague–Dawley rats we report alterations in behavioral pain thresholds following cessation of treatment that persisted into adulthood, which is accompanied by changes in the classification of dorsal root ganglia (DRG) sensory neurons and alterations in sensory nerve fiber termination in the skin and spinal dorsal horn (DH).

housed with their mother and littermates until P21 when they were weaned. Post-weaning rats were housed in single-sex cages of six animals with access to food and water *ab libitum*. Experimenters were blinded to all treatment groups at all stages.

Nociceptive behavioral experiments

Pups of both genders were randomly assigned to two groups, vehicle ($n = 22$) and cisplatin ($n = 19$) at birth (Postnatal (P) 0). Animals were treated with experimental agents from P7. The vehicle group were administered PBS (phosphate-buffered saline) and the treatment group administered cisplatin (1mg/kg dissolved in PBS) intraperitoneal (i.p.) injections once a day for five consecutive days (Fig. 1A) in two cohorts. In reference to human cisplatin administration, a single cycle of cisplatin treatment (typically between 60 and 100 mg/m², every ~3 weeks (Zsiros et al., 2010), with for example hepatoblastoma patients 19.1 months old (median age) receive 70 mg/m²/cycle patients (Zsiros et al., 2013). The dose of cisplatin used in this study is comparable to adult rodent studies which demonstrate sensory neuropathy (Park et al., 2013; Uhelski et al., 2015). One cohort was terminated at P16 (Immature) (vehicle ($n = 8$) and cisplatin ($n = 11$) the remainder remained in the study until P45 (adult). Prior to behavioral testing animals were habituated to handling and the room in which testing occurred. Mechanical withdrawal threshold and withdrawal latency to heat were measured as previously described (Vencappa et al., 2015). Mechanical threshold was measured using von Frey filaments (Linton), which were applied to the dorsal surface of the left and right hind paw of pups (<P21) or the plantar surface in older ani-

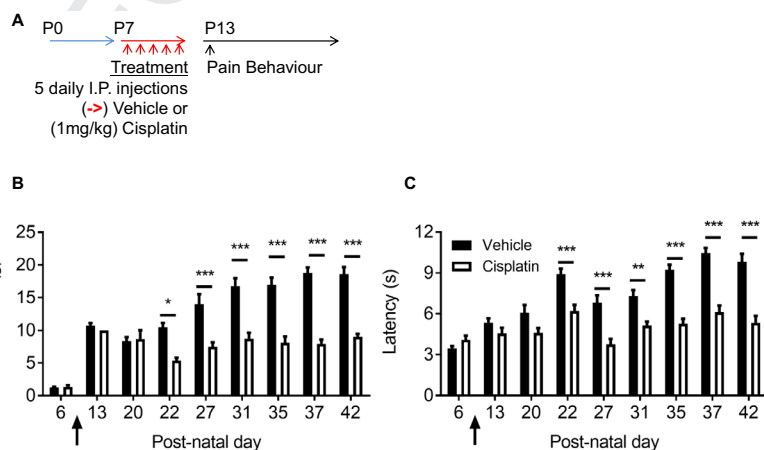


Fig. 1. Cisplatin treatment results in a delayed mechanical and thermal hypersensitivity. [A] P7 rats were treated with either i.p. injections of vehicle or cisplatin (1 mg/kg) for 5 consecutive days. [B] Experimental groups of animals did not display any alterations in mechanical withdrawal threshold between P6 and P20. However, from P22 to the end of the experiment the cisplatin-treated animals displayed a reduction in withdrawal threshold to mechanical stimulation when compared to vehicle injection ($P < 0.05$, $***P < 0.001$ Two ANOVA with post Bonferroni test; vehicle = 7, cisplatin $n = 5$). [C] In response to heat, animals from both experimental groups demonstrated similar withdrawal latencies. At P22 cisplatin-treated animals displayed a reduction in withdrawal latency to heat stimulation ($**P < 0.01$, $***P < 0.001$ Two ANOVA with post Bonferroni test; vehicle = 7, cisplatin $n = 5$).

EXPERIMENTAL PROCEDURES

Animals

Time mated pregnant Wistar rat dams were bought from Charles River UK. They were received into The University of Nottingham Biological Services Unit at E17 and allowed to habituate prior to parturition. Experiments were conducted under UK Home Office regulations and in concordance with the Animal (Scientific Procedures) Act (1986) and adhered to the ARRIVE Guidelines. Ethical approval was granted by the University of Nottingham Animal Welfare and Ethical Review Board. Animals were housed in light/dark (12:12 h) cycled rooms. Pups were

143 mals (>P21). Each hair (expressed in grams) was
 144 applied sequentially, five times each to determine
 145 mechanical force withdrawal thresholds which was deter-
 146 mined as the first hair to elicit a withdrawal response in
 147 40% of applications. Latency (seconds) to withdraw from
 148 a thermal stimulus was achieved using the plantar test
 149 (Hargreaves Apparatus, Ugo Basile). Thermal stimuli
 150 were applied to both feet three times, with a rest period
 151 between stimulations to avoid sensitization and the mean
 152 latency to the three presentations calculated.

153 Immunohistochemistry

154 Animals were terminally anesthetized with sodium
 155 pentobarbital (60 mg/ml; i.p.). The heart of each animal
 156 was exposed and blood collected from the left ventricle
 157 via cardiac puncture into heparinized tubes and stored
 158 at 4 °C. Animals were then perfused transcardially via
 159 this cannula with ice-cold PBS (> 100 ml) followed by
 160 4% paraformaldehyde (PFA; >200 ml). Tissue (spinal
 161 cord, L3-5 dorsal root ganglia (DRG), plantar hindpaw
 162 skin-full plantar width skin biopsies were extracted from
 163 mid-point of the heel to the proximal border of the
 164 footpad (excluding footpads Thakur et al., 2012) was
 165 collected and submerged in 4% PFA and left overnight
 166 at 4 °C. Tissues were then transferred to a 30% sucrose
 167 (in Phosphate buffer saline (PBS)) solution, kept at 4 °C
 168 overnight. Samples were then frozen in optimum cutting
 169 temperature (OCT) solution and stored at –80 °C until
 170 needed. Sections were cut using a cryostat and mounted
 171 on a Superfrost Plus slides (VWR International) and
 172 stored at –80 °C. Dorsal root ganglia were cut at 6 μm,
 173 plantar skin 20-μm thickness and spinal cord 40 μm.

174 Slides were placed in a humidified chamber and
 175 washed with PBS solution (3 times for 5 min each) and
 176 then with PBS 0.2% Triton x-100. Slides were incubated
 177 in blocking solution (PBS 0.2% Triton x-100 5% Bovine
 178 Serum Albumin (BSA) 10% Fetal Bovine Serum (FBS))
 179 for 30 min at room temperature. Primary antibodies
 180 were made up at required concentration in blocking
 181 solution. Antibodies, concentrations, sources are: mouse
 182 anti-NeuN (Millipore) (1 in 100), Rabbit anti-protein gene
 183 product 9.5 (PGP9.5) (Millipore, 1 in 200), Rabbit anti-
 184 calcitonin gene related peptide (CGRP) (Sigma, 1 in
 185 5000), mouse anti-Neurofilament 200 (NF200) (Sigma, 1
 186 in 1000), goat anti-tropomyosin receptor kinase A (TrkA)
 187 (R&D Systems, 1 in 100), rabbit anti-cleaved caspase 3
 188 (Cell Signalling, 1 in 500). These were incubated
 189 overnight at 4 °C. Slides were then washed a further 3
 190 times (5 min) in PBS. In some cases biotinylated
 191 antibodies were used (biotinylated donkey anti rabbit
 192 and biotinylated donkey anti goat, Jackson, 1 in 500).
 193 These were made up in PBS 0.2% Triton x-100 was
 194 pipetted to slides and left at room temperature for 2 h.
 195 These were washed 3 times (5 min) in. Slides were then
 196 incubated in Alexafluor antibody (Invitrogen, 1 in 1000)
 197 diluted appropriately in PBS 0.2% triton x-100 and were
 198 left in a dark environment at room temperature for 2 h.
 199 Alexafluors used were anti-mouse 488, streptavidin 555,
 200 streptavidin 405, and anti-rabbit 555. These were
 201 washed 3 times (5 min) in PBS. Slides were
 202 coverslipped (22 × 50 mm) using Fluorsave (Millipore).

Fluoroshield with DAPI (Millipore) was used for the
 plantar skin sections. Coverslips were sealed and stored
 at 4 °C in the dark. Slides were imaged using a Leica
 SPE confocal microscope and Leica Application Suite
 Software (TVBL imaging facility). Each DRG section
 was imaged in its entirety and for the plantar skin slides
 4–6 random images were taken per section to provide a
 representation. The x10 objective was used to image
 the DRGs and plantar skin sections for quantitative
 analysis and the x63 objective was used to generate
 high magnification images.

Spinal cords were cut at 40 μm using a microtome and
 left in sucrose azide (0.04% %) overnight. Sucrose azide
 was removed by washing in PBS (3× for 5 min). Slides
 were incubated with 3% blocking solution (0.1 M PBS,
 3% goat or donkey serum, 0.3% triton X-100) for one
 hour at room temperature. Primary antibodies, sources,
 concentrations and incubation times are: mouse anti
 NeuN (Millipore, 1 in 500), rabbit anti-GFAP (AbCam, 1
 in 500, Goat anti-TrkA (R&D Systems) (1 in 100),
 overnight. (Donkey anti-goat biotin (1 in 500) 2 h),
 Mouse anti-NF200 (Sigma) (1 in 750) 24 h, Rabbit anti-
 VGLUT2 (Synaptic Systems) (1 in 750) 24 h. The slides
 were then washed in PBS 5× for 10 min. Life
 technologies alexafluors used were; Streptavidin 405
 (1 in 1000), anti-mouse 488 (1 in 500), anti-rabbit 555
 (1 in 500). Samples were incubated for 2 h at room
 temperature in the dark, before washing in PBS 5× for
 10 min. Sections were mounted on gelatinized slides
 and allowed to dry overnight in the dark. Slides were
 coverslipped (22 × 50 mm) using Fluomount (Sigma),
 sealed and stored in the dark at 4 °C. Slides were
 imaged using a Leica SPE confocal microscope and
 Leica Application Suite Software (TVBL imaging facility),
 the dorsal horn of the spinal cord was imaged using the
 ×10 objective.

239 Analysis

Analysis was completed using Microsoft Excel and
 GraphPad Prism v 6.0 software. All data are presented
 as mean ± SEM. The area per field of view is 1.10 mm
 × 1.10 mm at ×10 magnification. Neuronal number and
 section area (μm²) were quantified automatically using
 Image J software region of Interest (ROI) manager tool
 (<http://imagej.net/Welcome>). IB4⁺, CGRP⁺, TrkA⁺ and
 NF200⁺ neurons were calculated as a percentage of
 the total DRG number (NeuN⁺/PGP9.5⁺ stained). Total
 DRG neuronal number was determined from using
 PGP9.5 and NeuN co-staining and quantified per ROI
 (whole DRG section). A minimum of 10 sections per
 animal used and mean total sensory neuron count per
 DRG was determined. It was determined that the total
 neuronal number for PGP9.5 and NeuN was similar
 between treatment groups (Fig. 5). IENF density were
 quantified, using image J software, as fibers entering
 the epidermis (visualized with DAPI/dotted white line).
 Numbers were normalized for epidermal length (μm)
 and to the mean of vehicle animals. Five random
 images were acquired per plantar skin sample per
 animal with a minimum of 10 sections per animal used.
 From these the average IENF density score was

263 calculated per animal. A minimum total of 7400 DRG
 264 sensory neurons and 2100 IENF were analyzed over
 265 the complete study. All DRG and IENF analysis
 266 previously described (Hulse et al., 2015). Unpaired T test
 267 was performed on the percentage DRG number and total
 268 IENF density from plantar skin. Two-way ANOVA with
 269 post hoc Bonferroni test was performed for DRG sensory
 270 neuronal soma area analysis. Images of the spinal cords
 271 were acquired and analyzed using the region of interest/
 272 plot profile plugin in Image J. A total of 4 random regions
 273 of interest were calculated and calibrated to depth of sec-
 274 tion. Area under the curve (AUC) analysis and an
 275 unpaired T Test were performed to determine dorsal horn
 276 innervation. Nociceptive behavioral testing was analyzed
 277 using a two-way ANOVA with post hoc Bonferroni test.

278 In the spinal cord stains: CGRP, IB4, TrkA, NF200
 279 and vGLUT2 staining was analyzed by plotting four lines
 280 of interest through each image in ImageJ to measure
 281 gray value (AU) intensity using the plot profile tool. Each

straight plot line (fixed width) extended ventrally 600 μm ,
 from the outer dorsal surface of sections/outer region of
 lamina I, to lamina V of the dorsal horn. The origin of
 each line was equally spaced following the outer curve
 of the dorsal horn using a similar method as previously
 described (Lorenzo et al., 2008). Results for each group
 were averaged to give a single intensity profile for cis-
 platin and vehicle groups. The area under the curve
 (AUC) was taken for the averaged intensity profile to cre-
 ate a figure for the entire dorsal horn. Results were tested
 for parametric normality with D'Agostino and Pearson
 omnibus normality test. Cisplatin and vehicle cell counts
 were compared and analyzed for statistical significance
 using an unpaired T-test with Kolmogorov–Smirnov post
 hoc test. In the spinal cord NeuN and GFAP cell counts
 were taken from five 100 $\mu\text{m} \times 100 \mu\text{m}$ regions of interest
 (ROI) for lamina I, II and V of the dorsal horn, using the
 ROI manager plugin on ImageJ. Results for each group,
 were averaged to give a single cell count for each lamina,

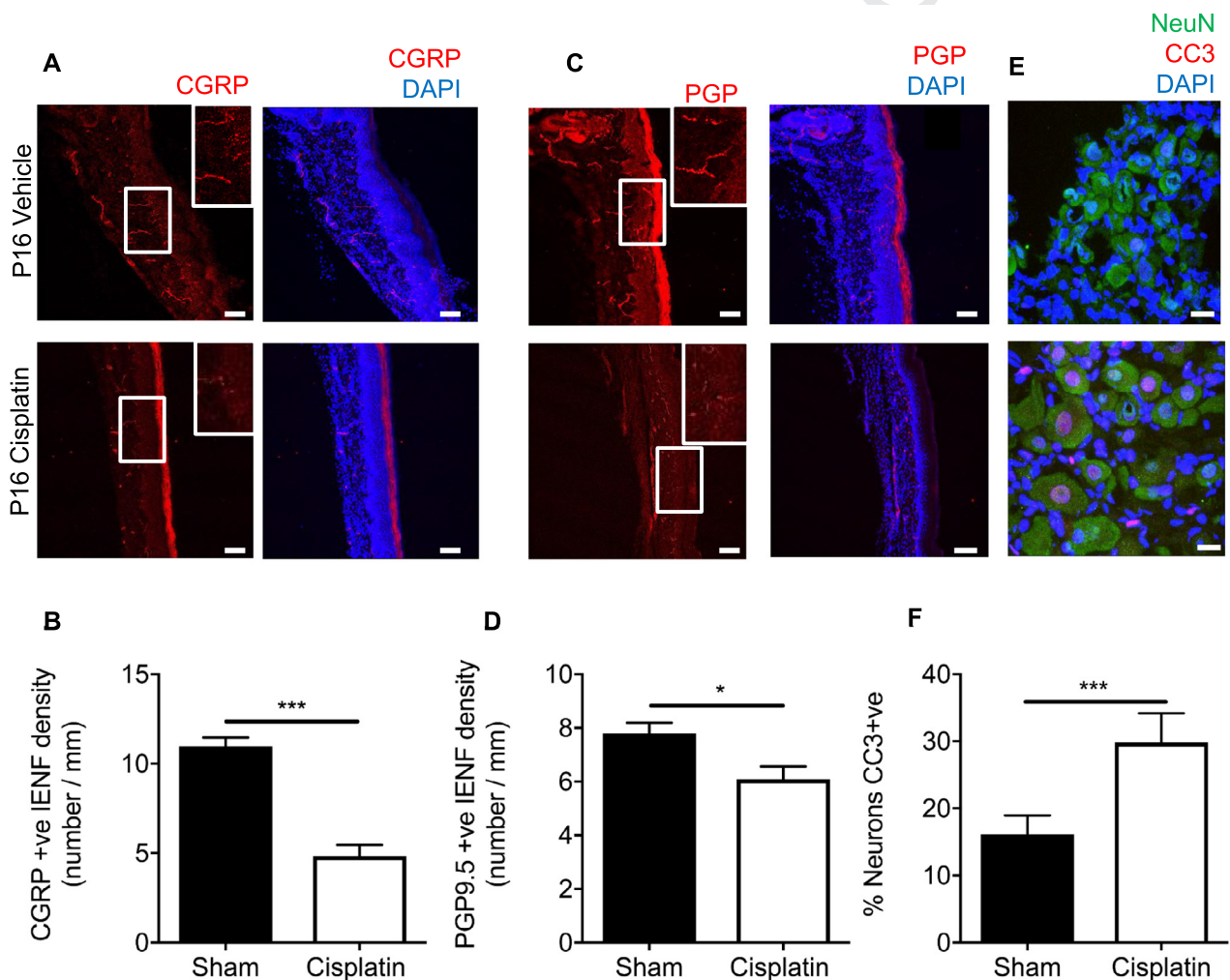


Fig. 2. Cisplatin treatment leads to sensory neurodegeneration. IENF measurements were taken from the hindpaw plantar skin from P16–20 rats treated with either vehicle or cisplatin. [A&B] There was a reduction in CGRP +ve IENF in the plantar skin of cisplatin animals versus vehicle (IENF/mm, $^{***}P < 0.01$ Unpaired T test; vehicle = 4, cisplatin $n = 4$; scale bar = 100 μm). [C&D] PGP9.5 +ve IENF was also reduced in cisplatin-treated animals when compared to vehicle (IENF/mm, $^{*}P < 0.05$ Unpaired T test; vehicle = 4, cisplatin $n = 4$; scale bar = 100 μm). [E&F] L4 Sensory DRG neurons were collected from both experimental groups; vehicle and cisplatin at P16–20. Cleaved caspase 3 (CC3) was increased in DRG sensory neurons (NeuN +ve) in the cisplatin-treated animals versus vehicle rats ($^{*}P < 0.05$ Unpaired T test; vehicle = 4, cisplatin $n = 4$; scale bar = 20 μm).

301 and then for the entire dorsal horn section to identify total
 302 neuron or astrocyte number per dorsal horn of spinal cord
 303 and of the designated laminae. Results were tested for
 304 parametric normality with D'Agostino and Pearson
 305 omnibus normality test. Cisplatin and vehicle cell counts
 306 were compared and analyzed for statistical significance
 307 using an unpaired *T*-test with a Mann–Whitney test.
 308 *P* values are represented as **P* < 0.05, ***P* < 0.01 and
 309 ****P* < 0.001. NS dictates not significant.

RESULTS

Early-life cisplatin exposure leads to a delayed onset of mechanical and thermal hypersensitivity

310
 311 To assess whether cisplatin treatment results in sensory
 312 abnormalities when administered in early-life daily
 313
 314

315 intraperitoneal injections of either vehicle (PBS) or
 316 Cisplatin (1mg/kg) starting on day P7, were performed
 317 for 5 consecutive days. Cisplatin-treated animals
 318 developed a persistent but delayed (onset P22)
 319 mechanical hypersensitivity compared to vehicle-treated
 320 rats, (Fig. 1B; **P* < 0.05, ****P* < 0.001 Two-way ANOVA
 321 with post Bonferroni test) and this difference between
 322 the two groups was maintained until the end of the
 323 experiment (P42; Vehicle = 18.58 ± 1.09 g vs Cisplatin
 324 = 9.03 ± 0.42 g). Heat hypersensitivity also developed
 325 in the cisplatin group, with persistently shorter
 326 withdrawal latencies evident from P22 to the end of the
 327 study (P42; Vehicle = 9.82 ± 0.58 s vs Cisplatin = 5.3
 328 4 ± 0.51 s) when compared to the vehicle treatment
 329 group (Fig. 1C; ***P* < 0.01, ****P* < 0.001 Two-way
 330 ANOVA with post Bonferroni test).

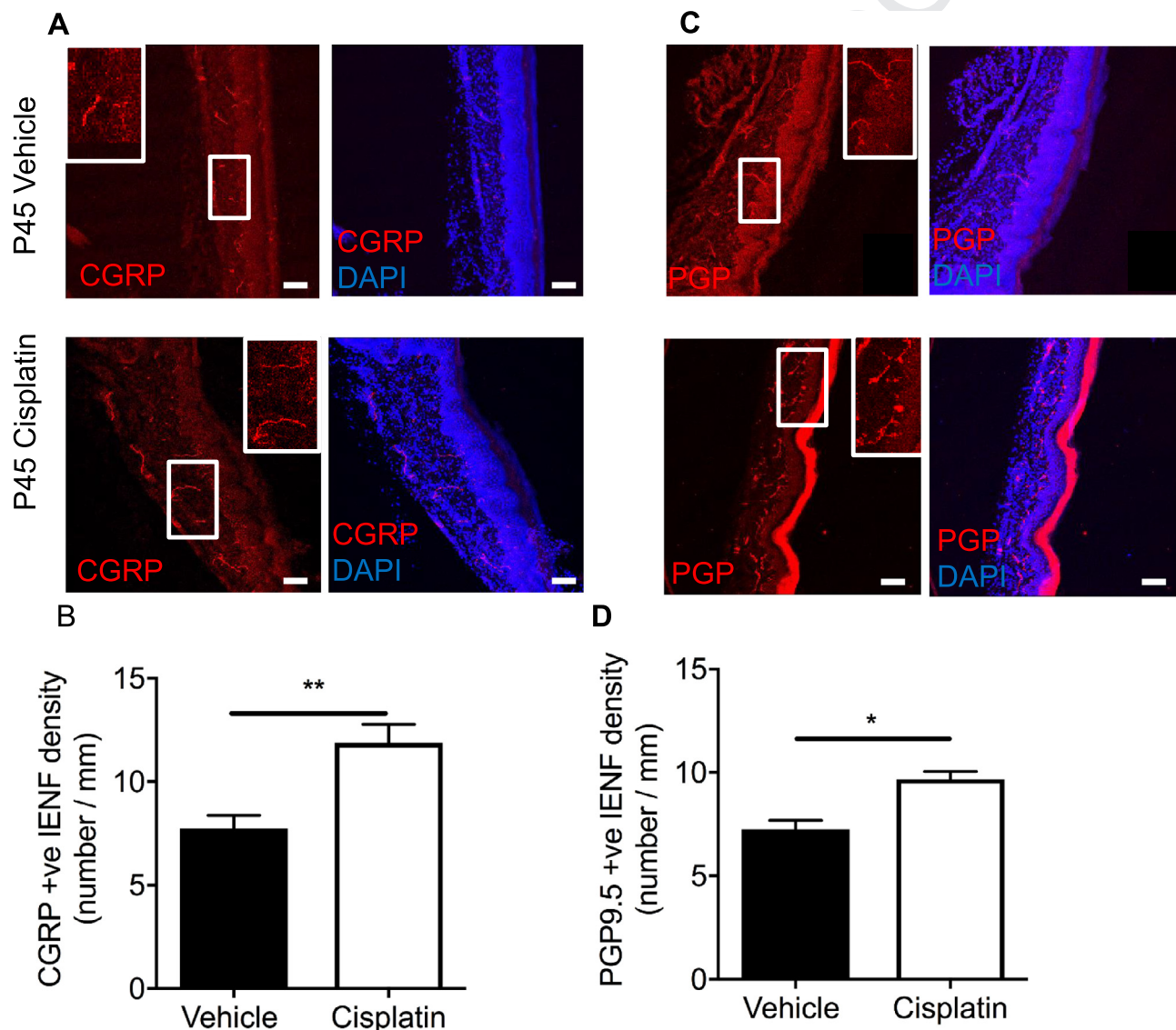


Fig. 3. Cessation of cisplatin treatment induces neuroregeneration in adults. CGRP+ve and PGP+ve IENF were measured in the plantar skin taken from hindpaws of both experimental groups; vehicle and cisplatin at P45. [A&B] In the cisplatin-treated animals there was an increase in CGRP+ve IENF versus the vehicle groups (IENF/mm, ***P* < 0.01 Unpaired T test; vehicle = 5, cisplatin *n* = 5). [C&D] Similarly, PGP+ve IENF was also increased in the plantar skin of cisplatin-treated animals when compared to vehicle-treated animals (IENF/mm, **P* < 0.05 Unpaired T test; vehicle = 5, cisplatin *n* = 5) (scale bar = 100 μm).

Cisplatin treatment leads degeneration of the peripheral nervous system

Cisplatin is a widely used cancer chemotherapeutic, which in adults induces sensory neurodegeneration (Ta et al., 2006; Mao-Ying et al., 2014). Intraepidermal nerve fiber (IENF) density in the plantar skin and dorsal root ganglia sensory neuron number were measured in vehicle and cisplatin-treated animals a week (P16) post termination of treatment. Cisplatin exposure led to a reduction in the number of CGRP positive (Fig. 2A, B; $**P < 0.01$ Unpaired T test; Vehicle = 10.98 ± 0.39 IENF/mm vs Cisplatin = 4.93 ± 1.44 IENF/mm) and PGP9.5 positive (Fig. 2C&D; $P < 0.05$ Unpaired T test; Vehicle = 7.98 ± 0.62 IENF/mm vs Cisplatin = 6.08 ± 0.32 IENF/mm) IENFs in the plantar skin versus vehicle controls. At this timepoint there were significantly more L4 DRG neurons positive for cleaved caspase 3 (CC3) in the cisplatin group when compared to vehicle animals (Fig. 2E&F; $**P < 0.01$ Unpaired T test; Vehicle = $15.82 \pm 3.43\%$ vs Cisplatin = $29.89 \pm 1.49\%$). When pups were allowed to mature to P45 following treatment with cisplatin between P7-11

we observed a significant increase in the number of CGRP (Fig. 3A, B, $**P < 0.01$ Un-paired T-test; Vehicle = 7.76 ± 0.62 IENF/mm vs Cisplatin = 11.88 ± 0.90 IENF/mm) positive and PGP9.5 (Fig. 3C, D, $*P < 0.05$ Un-paired T-test; Vehicle = 7.25 ± 0.43 IENF/mm vs Cisplatin = 9.69 ± 0.36 IENF/mm)-positive IENF in plantar hindpaw skin compared to controls.

Cisplatin has no effect on DRG cell populations immediately following treatment

L4 DRG neurons extracted from vehicle and cisplatin-treated animals aged P16 were stained for pan-neuronal markers (Fig. 4) NeuN and PGP9.5. Sensory neurons are often categorized on the basis of their expression of neuropeptides (e.g. CGRP), lack of neuropeptides (IB₄) or markers of myelination (NF200). Sensory DRG neurons were labeled with (Fig. 4A) CGRP and (Fig. 4B) IB₄, in addition to pan-neuronal marker (Fig. 4C) NeuN. The percentage of specific sensory neuronal subsets for (Fig. 4D) CGRP (Vehicle = 53.1 ± 1.47 vs Cisplatin = 59.72 ± 2.09) and (Fig. 4E) IB₄ (

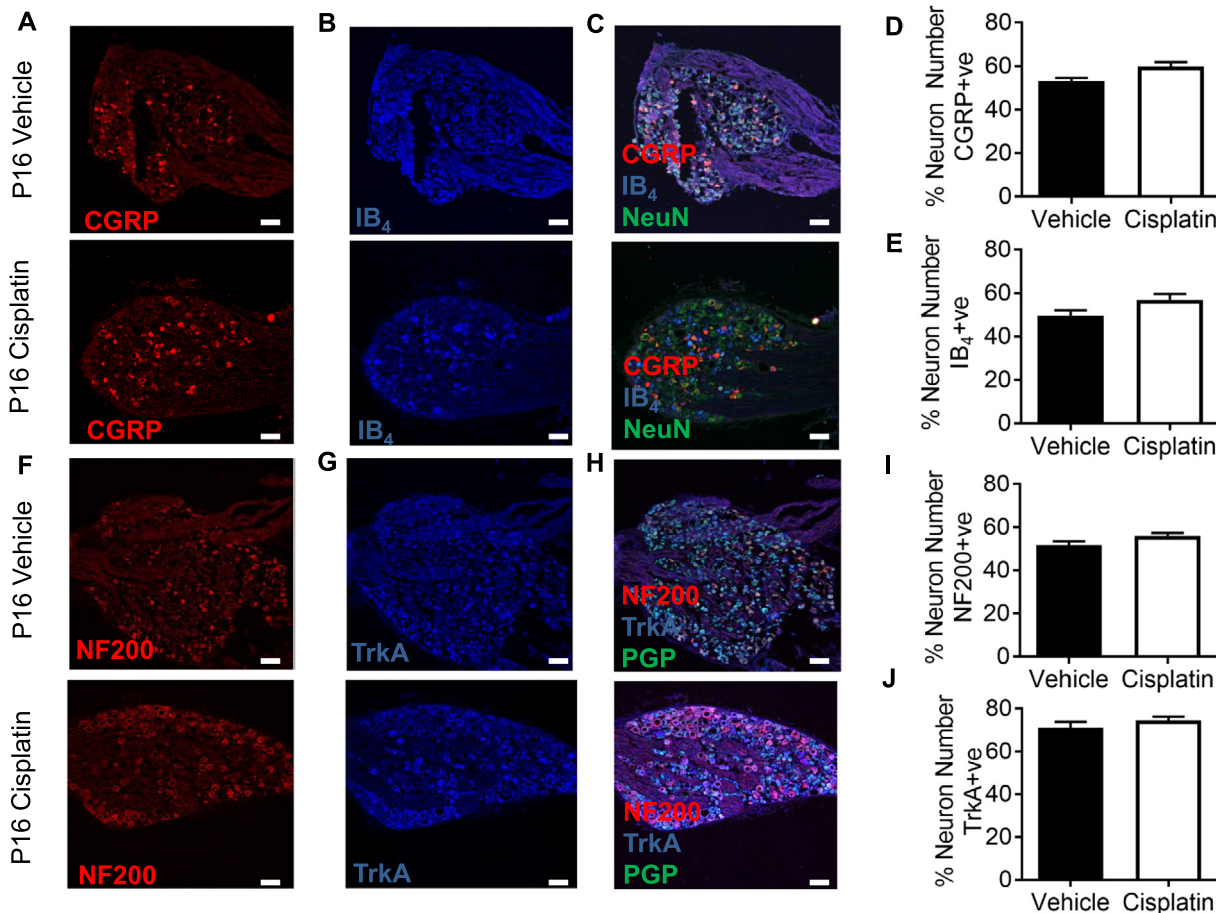


Fig. 4. Cisplatin does not alter sensory neuronal delineation. Sensory DRG neurons were stained for [A] CGRP and [B] IB₄ to represent the small diameter DRG sensory neuron populations in both vehicle and cisplatin-treated P16 animals. These were co-localized with [C] NeuN. There were no differences between experimental groups in the percentage of [D] CGRP and [E] IB₄ (non-peptidergic) sensory DRG neuronal subclasses. In addition, DRG sensory neurons were labeled for the myelinated sensory neuronal marker [F] NF200 and the small diameter neuronal marker [G] TrkA (peptidergic) in vehicle and cisplatin-treated P16 animals. These were co-localized with [H] PGP9.5. There were no differences between groups in the percentage of the [I] NF200 or [J] IB₄ sensory DRG neuronal subclasses (vehicle = 4, cisplatin n = 4; scale bar = 50 μm).

372 Vehicle = $49.53 \pm 2.53\%$ vs Cisplatin = 56.86 ± 2.63)
 373 was unchanged between experimental groups. Sensory
 374 DRG neurons extracted from age-matched vehicle and
 375 cisplatin-treated animals aged P16 were labeled with
 376 (Fig. 4F) NF200 and (Fig. 4G) TrkA, in conjunction with
 377 a pan neuronal marker, (Fig. 4H) PGP9.5. The
 378 percentage of total sensory neurons labeled with either
 379 (Fig. 4I) NF200 (Vehicle = $51.58 \pm 1.85\%$ vs Cisplatin
 380 = 55.91 ± 1.39) or (Fig. 4J) TrkA (Vehicle = 71.03 ± 2
 381 $.87\%$ vs Cisplatin = 74.53 ± 1.73) were unchanged
 382 between vehicle and cisplatin-treated groups at P16.

383 Cisplatin leads to long-term re-organization of the 384 peripheral nervous system

385 We next assessed whether there were any delayed
 386 effects of neonatal cisplatin treatment upon DRG
 387 composition in rats at P45. We found that there were no
 388 significant differences in the total number of DRG
 389 sensory neurons in either experimental group at P45
 390 (Total DRG sensory neuron number Fig. 5A, B; NeuN;
 391 NS Unpaired T test; (Vehicle = 64.05 ± 5.19 vs Cispla

tin = 67.41 ± 4.83), Fig. 5C, D; PGP9.5; NS Unpaired
 392 T test; (Vehicle = 60.59 ± 7.57 vs Cisplatin = $63.72 \pm$
 393 8.01), as well as no difference in size profiles of the
 394 DRG neurons (Fig. 5E PGP9.5+ve; NS Two-way
 395 ANOVA with post hoc Bonferroni; NeuN size profile NS
 396 Two-way ANOVA with post hoc Bonferroni, data not
 397 shown) between experimental groups at P45.
 398 Representative images of NeuN and PGP9.5 co-
 399 localization in DRG neurons (Fig. 5F) and no primary
 400 controls (Fig. 5G; cells positive for DAPI).

402 At P45 the total number of sensory DRG neuronal
 403 subsets was calculated (Fig. 6A; co-labeled with NeuN)
 404 with the total number of (Fig. 6B) CGRP and (Fig. 6C)
 405 IB₄-positive neurons determined. Representative merge
 406 image of NeuN, CGRP and IB₄-positive sensory DRG
 407 neurons (Fig. 6D). There were no significant changes in
 408 the total number of CGRP+ve (Fig. 6E; NS Unpaired T
 409 test; (Vehicle = 20.83 ± 0.83 vs Cisplatin = $19.67 \pm$
 410 1.04%) and IB₄+ve (Fig. 6F; NS Unpaired T test;
 411 (Vehicle = 28.27 ± 2.34 vs Cisplatin = 30.35 ± 1.15))
 412 in either vehicle or the cisplatin-treated group.
 413 Furthermore, DRG sensory neurons (PGP9.5+ve

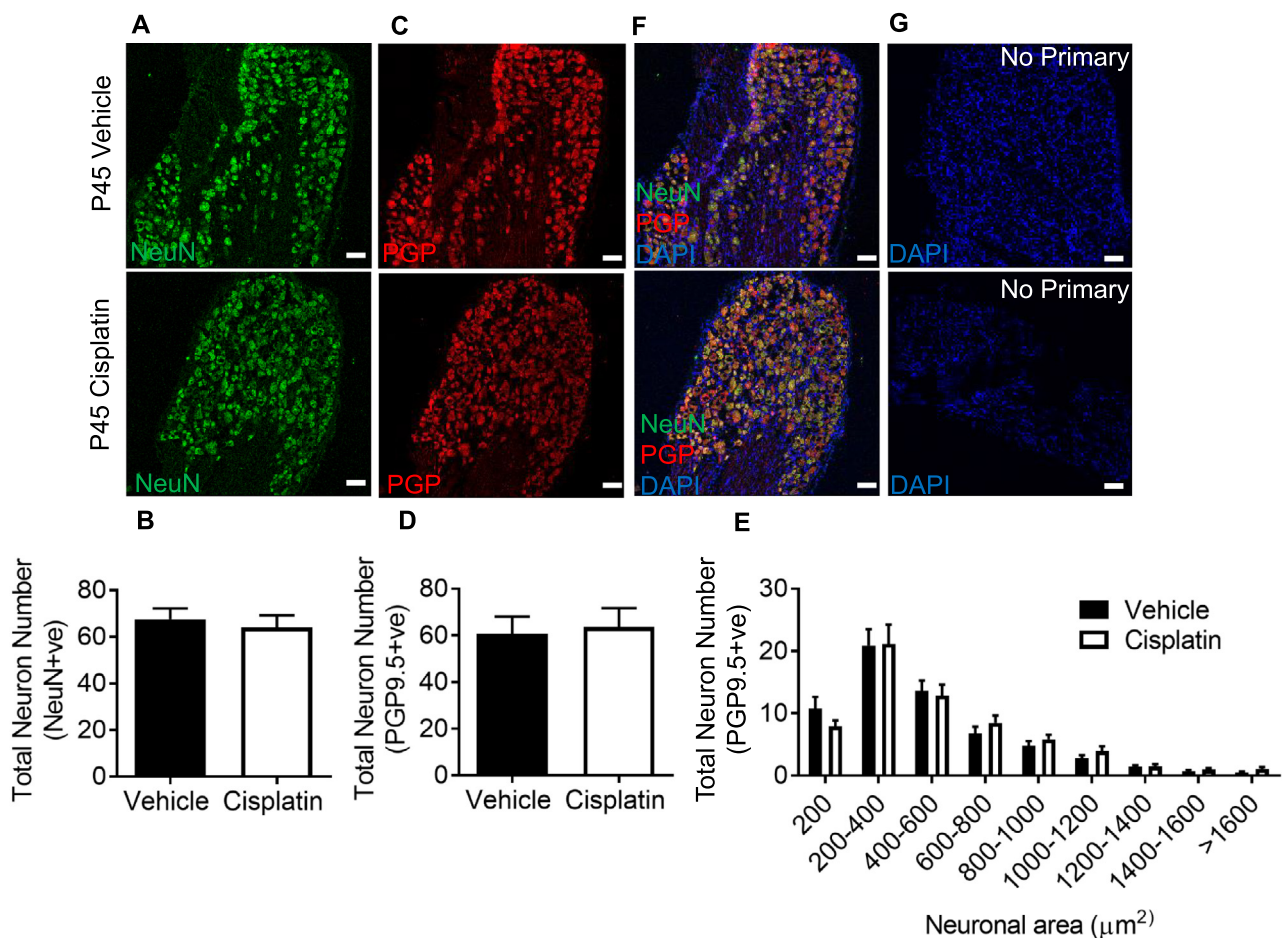


Fig. 5. The effect of cisplatin treatment on DRG sensory neurons. DRG sensory neurons were counted from both experimental groups (vehicle and cisplatin treated) at the timepoint P45. DRG neurons were stained for NeuN and PGP9.5. There was no difference in the total number of L4 DRG sensory neurons ([A–B] NeuN + ve and [C–D] PGP9.5). [E] DRG neuron size profile demonstrating no change in neuron number per designated neuronal soma area. Representative image of co-staining with [F] NeuN and PGP9.5 and of [G] no primary controls (vehicle = 5, cisplatin $n = 5$) (scale bar = 100 μm).

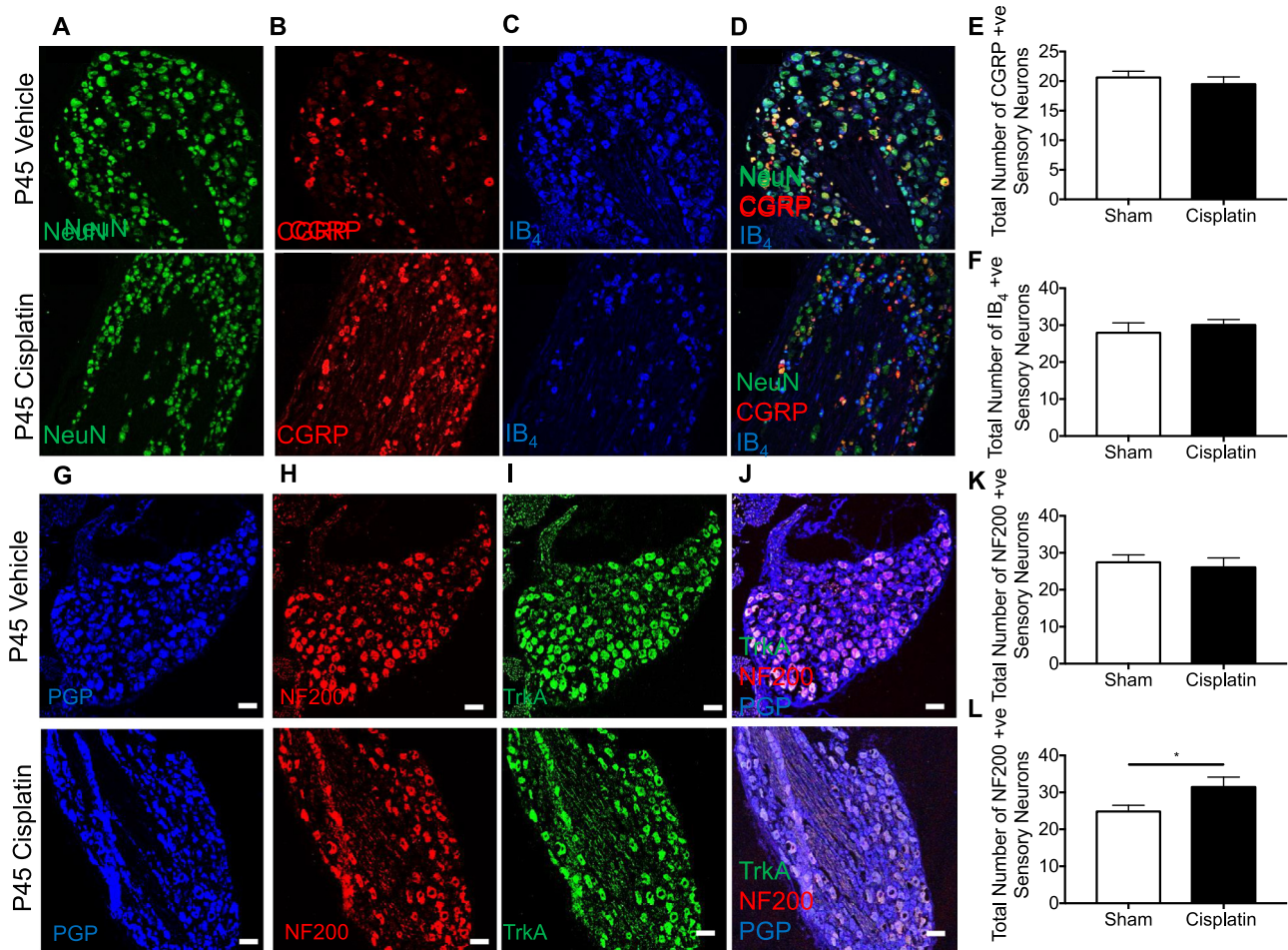


Fig. 6. The effect of cisplatin treatment on DRG neuron subclass expression in adults. Sub-classifications of L4 DRG sensory neurons were investigated in P45 animals in both vehicle and cisplatin groups. Total numbers of sensory DRG neurons were determined with [A] NeuN. Small diameter sensory DRG neurons were labeled with [B] CGRP and [C] IB₄. [D] Merged representation of NeuN, CGRP and IB₄. There were no differences between experimental groups (age-matched vehicle and cisplatin) in the total number of neurons expressing [E] CGRP or [F] IB₄. Total numbers of sensory DRG neurons were determined with [G] PGP9.5 when sensory DRG neurons were labeled for the myelinated sensory neuronal marker [H] NF200 and small diameter sensory neuronal marker [I] TrkA. [J] Representative image of colocalized TrkA or NF200 with PGP9.5. There were no differences between experimental groups (age-matched vehicle and cisplatin) in the total number of sensory neurons expressing [K] NF200. However, there was an increase in the percentage of DRG neurons expressing [L] TrkA in the cisplatin group ($P < 0.05$ Unpaired T test; vehicle = 5, cisplatin $n = 5$) (scale bar = 100 μm).

414 co-labeled Fig. 6G) labeled for (Fig. 6H) NF200+ve or
415 (Fig. 6I) TrkA (Fig. 6J; representative merge image of
416 PGP9.5, NF200 and TrkA-positive sensory DRG
417 neurons) demonstrated there (Fig. 6K; NS Unpaired

Table 1. The effect of cisplatin treatment on DRG neuron subclass expression in adults. Total number of sensory DRG neurons expressing CGRP, IB₄, NF200 or TrkA were determined in experimental groups vehicle and cisplatin treat at P45 of age. ($P < 0.05$ Unpaired T test; vehicle = 5, cisplatin $n = 5$)

	Vehicle	Cisplatin
	% Total Sensory Neuron Number (Mean \pm SEM)	% Total Sensory Neuron Number (Mean \pm SEM)
CGRP	30.88 \pm 1.24	30.71 \pm 1.63
IB ₄	41.88 \pm 3.46	47.39 \pm 1.79
NF200	41.05 \pm 2.59	41.12 \pm 3.49
TrkA	37.20 \pm 2.09	49.59 \pm 3.67*

T test; Vehicle = 27.70 \pm 1.74 vs Cisplatin = 26.70 \pm 2.23) was no difference between the cisplatin-treated group and the vehicle-treated group at P45 for total number of NF200-positive neurons. However, there was a significant increase in the number of TrkA+ve DRG neurons in the cisplatin group vs the vehicle group (Fig. 6L; $*P < 0.05$ Unpaired T test; (Vehicle = 25.10 \pm 1.41 vs Cisplatin = 31.76 \pm 2.35) at P45. Percentage change in the sensory DRG neuron subsets are represented as a proportion of total sensory DRG neuron number (Table 1).

Early-life chemotherapy Results in immediate alterations in sensory neuron termination within the spinal dorsal horn

As well as innervating the skin, DRG neurons have a reciprocal termination with the spinal cord DH. The termination pattern of sensory neuron fibers within the

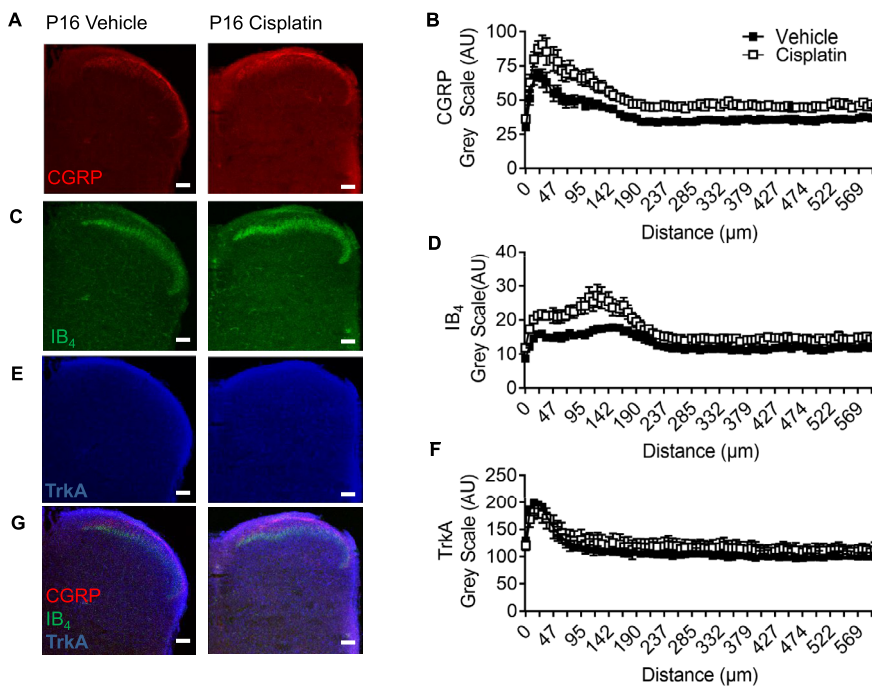


Fig. 7. Sensory nerve terminal innervation into dorsal horn is altered following cisplatin exposure. In cisplatin postnatal day 16 (P16) animals there was increased immunoreactivity in the superficial dorsal horn of [A–B] CGRP ($**p < 0.001$ Two-way ANOVA) and [C–D] IB₄ ($**p < 0.001$ Two-way ANOVA) compared to vehicle-treated age-matched rats. [E–F] TrkA distribution in the dorsal horn was unaltered between vehicle and cisplatin treatment groups. A merged representation of CGRP, IB₄ and TrkA is presented for [G] vehicle and cisplatin (vehicle = 4, cisplatin $n = 4$; scale bar = 100 μm).

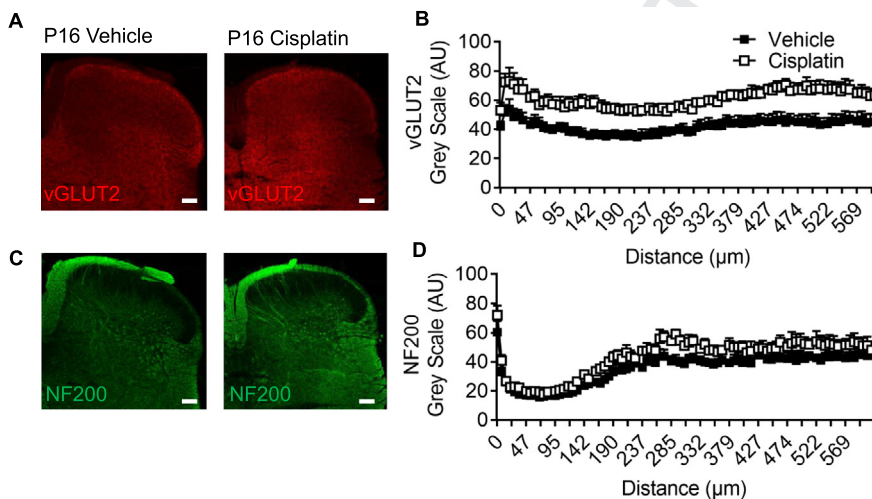


Fig. 8. Cisplatin induced reorganization of sensory nerve fiber innervation into the dorsal horn. In P16 cisplatin-treated animals [A–B] vGLUT2 sensory neuron innervation into the dorsal horn of the spinal cord was increased versus age-matched vehicle-treated rats ($*p < 0.05$; Two-way ANOVA). Additionally, there was no change in [C–D] NF200 immunoreactivity between the age-matched vehicle and cisplatin-treated P16 rats (vehicle = 4, cisplatin $n = 4$; scale bar = 100 μm).

There was an increase in CGRP (Fig. A-7B; (Vehicle = 39.64 ± 0.53 AUC vs Cisplatin = 52.02 ± 0.74AUC) $**P < 0.01$ Two-way ANOVA) and IB₄ (7C-D; (Vehicle = 13.08 ± 0.14 AUC vs Cisplatin = 17.22 ± 0.26AUC) $**P < 0.01$ Two-way ANOVA) immunoreactivity in the dorsal horn of cisplatin animals versus age-matched vehicle controls. Whereas there was no change for TrkA (Fig. 7E, F; (Vehicle = 112.1 ± 1.42AUC vs Cisplatin = 121.00 ± 1.07AUC)). Demonstration of colocalization and dorsal horn laminae of CGRP, IB₄ and TrkA in vehicle and cisplatin-treated animals (Fig. 7G). Additionally, vGLUT2 (Fig. 8A, B), which designates small diameter sensory neurons, demonstrated an increase in vGLUT2 immunoreactivity in the P16 cisplatin-treated animals (Fig. 8B; (Vehicle = 42.27 ± 0.36AUC vs Cisplatin = 61.32 ± 0.36AUC) $*P < 0.05$ Two-way ANOVA). Furthermore, NF200 (Fig. 8C, D) for myelinated primary sensory nerve afferents, there was no change in NF200 (Fig. 8B; (Vehicle = 35.65 ± 0.65AUC vs Cisplatin = 43.04 ± 0.79AUC)) in the dorsal horn of cisplatin-treated animals versus vehicle controls.

At P45 sensory nerve afferent terminals in the spinal cord were identified through immunoreactivity for (Fig. 9A) CGRP, (Fig. 9B) IB₄, and (Fig. 9C) TrkA. CGRP sensory inputs to the DH (Fig. 9E; (Vehicle = 42.9 ± 2.61AUC vs Cisplatin = 43.65 ± 3.08AUC) NS Two-way ANOVA) was unchanged, with similar intensity and depth of innervation into the dorsal horn between vehicle and cisplatin groups. There was a small increase in IB₄ staining in the dorsal horn of the spinal cord of cisplatin-treated animals (Fig. 9F; (Vehicle = 23.63 ± 0.90AUC vs Cisplatin = 27.87 ± 1.25AUC) $*P < 0.05$ Two-way ANOVA). There was an increase in TrkA immunoreactivity intensity and depth of innervation in the cisplatin group versus age-matched vehicle controls (Fig. 9G; (Vehicle = 53.23 ± 2.83AUC vs Cisplatin = 93.54 ± 4.46AUC) $**P < 0.01$ Two-way ANOVA; representative colocalization/dorsal laminae images Fig. 9G). Furthermore, vGLUT2 (Fig. 10A-B; (Vehicle = 19.75 ±

435 DH was investigated following the end of cisplatin
436 treatment (P16) with significant differences being
437 observed between the groups. Primary sensory nerve
438 afferent terminals in the spinal cord were identified
439 through immunoreactivity for CGRP, IB₄, and TrkA.

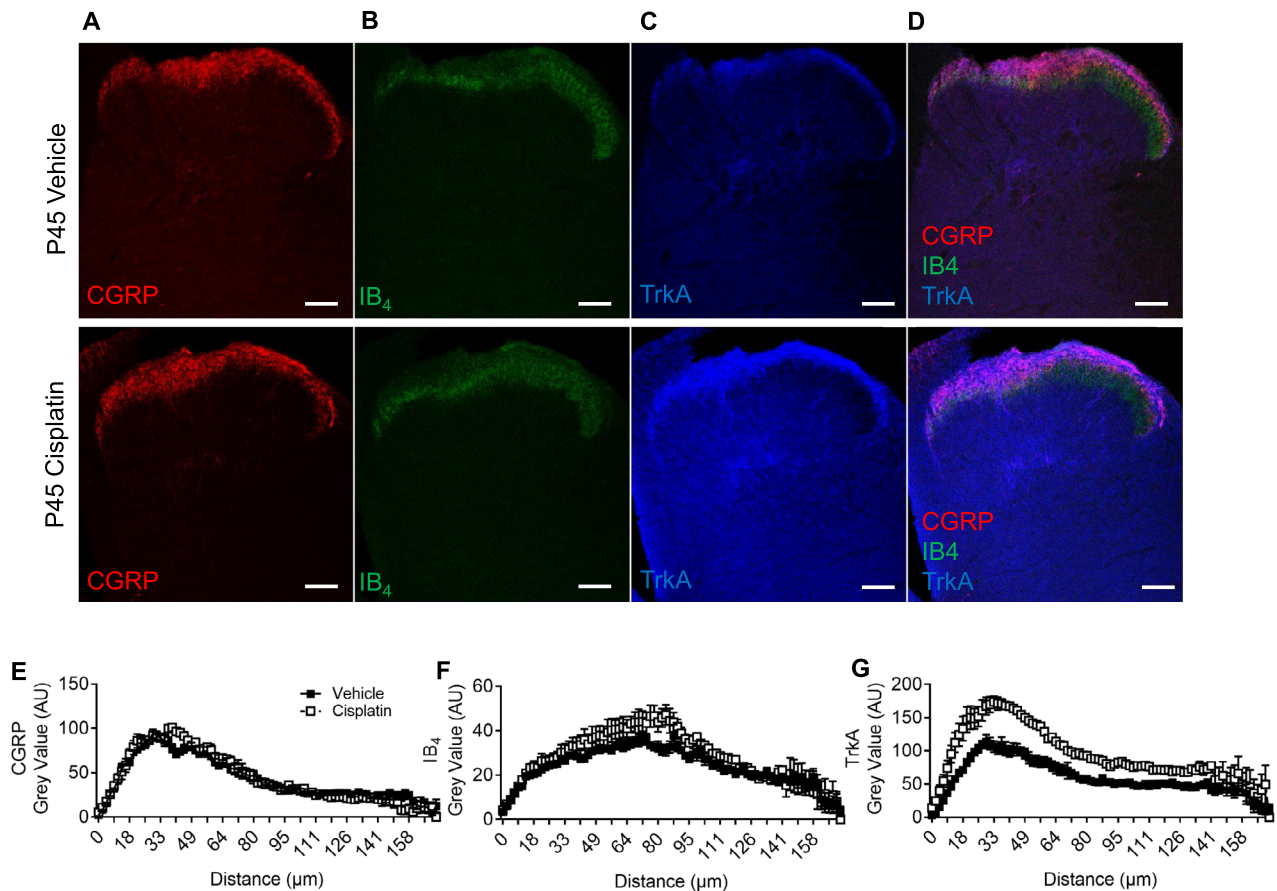


Fig. 9. Cisplatin treatment early in life leads to increased innervation of sensory afferent terminals in the superficial dorsal horn in adult rats. Sensory nerve fiber terminals within the dorsal horn of 45 day old rats (treated with either vehicle or cisplatin) were defined using [A] CGRP, [B] IB₄ and [C] TrkA immunoreactivity. [D] Representative overlay images of the dorsal horn displaying CGRP, IB₄ and TrkA nerve terminals in the vehicle and cisplatin groups. There was no change in the depth by which [E] CGRP + ve nerve fiber terminated in the dorsal and there was no change in the intensity within the dorsal horn in either experimental group (vehicle or cisplatin). [F] However, there was an increase in IB₄ intensity ($P < 0.05$ Two-way ANOVA; vehicle = 5, cisplatin $n = 5$) within the dorsal horn of cisplatin-treated animals compared to vehicle. [G] There was also an increase in intensity as well as depth of the TrkA +ve sensory nerve innervation in the dorsal horn of cisplatin-treated animals versus control. (** $P < 0.01$ Two-way ANOVA; vehicle = 5, cisplatin $n = 5$). Representative merge image of CGRP, IB₄ and TrkA and NF200 (scale bar = 100 μm).

501 0.17AUC vs Cisplatin = 44.01 \pm 0.29AUC) ** $P < 0.01$
 502 Two-way ANOVA) as well as NF200 (Fig. 10C-D; (Vehi
 503 cle = 18.04 \pm 0.43AUC vs Cisplatin = 36.2 \pm 0.92AU
 504 C) * $P < 0.05$ Two-way ANOVA; representative merge
 505 image Fig. 10E) input into the spinal cord was also
 506 increased in the cisplatin-treated animals.

507 Cisplatin-treated animals at P16 did not show any
 508 change in the number of NeuN-positive neuronal cell
 509 bodies (Fig. 11A–C; NS; Unpaired T test; (Vehicle = 19.
 510 18 \pm 4.49 vs Cisplatin = 18.58 \pm 3.98)) or GFAP
 511 expressing astrocytes (Fig. 11D–F; NS; Unpaired T test;
 512 (Vehicle = 7.08 \pm 0.19 vs Cisplatin = 6.79 \pm 0.32)) in
 513 the dorsal horn when compared to age-matched vehicle
 514 controls. At P45 cisplatin-treated animals did not show
 515 any change in neuron number (NeuN) (Fig. 11G–I; NS;
 516 Unpaired T test; (Vehicle = 16.8 \pm 3.60 vs Cisplatin =
 517 17.72 \pm 3.46)) or astrocyte number (GFAP) (Fig. 11 J-
 518 K; NS; Unpaired T test; (Vehicle = 2.88 \pm 0.38 vs Cispla
 519 tin = 3.18 \pm 0.23)) at P45 across the entire spinal cord

520 DH. However, in lamina V of the DH there was a
 521 significant increase in astrocyte expression of GFAP in
 522 cisplatin-treated adult rats (Fig. 11L; $P < 0.01$; Unpaired
 523 T test).

DISCUSSION

524
 525 Chemotherapy is crucial for the treatment of cancer.
 526 Improvements in basic research, diagnosis and the
 527 advancement of anti-cancer strategies, have led to a
 528 considerable improvement in cancer survival rates.
 529 However, as a consequence of this patients and families
 530 are commonly expected to deal with the adverse long-
 531 lasting side effects of treatment. Platinum-based drugs
 532 are widely used to treat cancers and are commonly
 533 associated with sensory neuropathy in adult patients.
 534 Unfortunately, many childhood cancers are also treated
 535 with such cytotoxic agents and they can have a
 536 devastating impact upon the development of the patient.

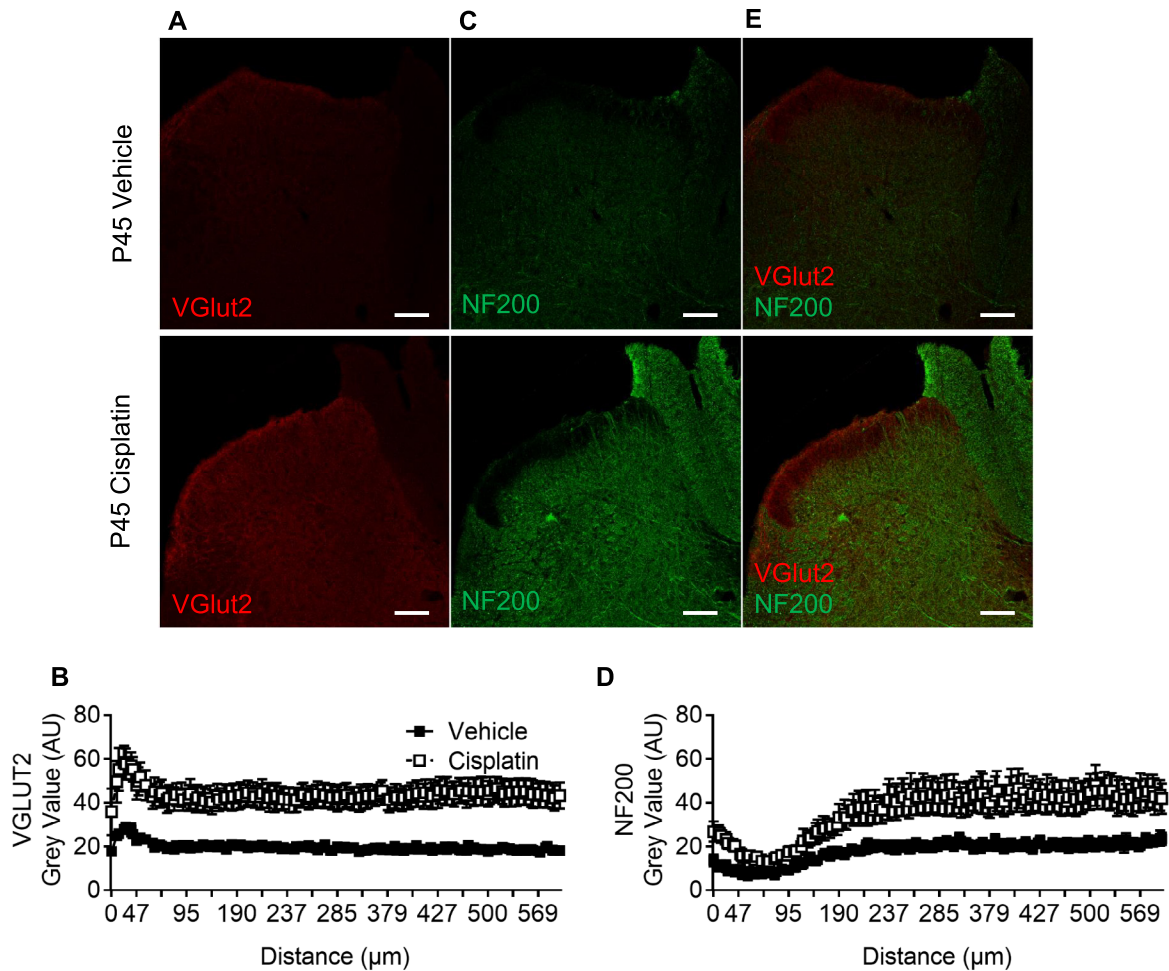


Fig. 10. Cisplatin treatment early in life leads to increased innervation of sensory afferent terminals in the superficial and deep dorsal horn in adult rats. [A] vGLUT2+ve sensory afferent nerve terminals were found to terminate in the superficial lamina (lamina I) in the vehicle group. However, [B] there is a wide spread increase in the cisplatin group when compared to vehicle animals ($**P < 0.01$ Two-way ANOVA; vehicle = 5, cisplatin $n = 5$). [C] NF200 immunoreactivity demonstrates [D] an increase in myelinated structures within the dorsal horn of the spinal cord of cisplatin animals versus the vehicle group ($*P < 0.05$ Two-way ANOVA; vehicle = 5, cisplatin $n = 5$). [E] Representative merge image of VGLut2 and NF200 (scale bar = 100 μm).

537 Although side-effects of treatment are well recognized
538 (e.g. difficulties in learning and social interactions,
539 hearing and vision (Grewal et al., 2010; Clanton et al.,
540 2011), there has been minimal investigation into the
541 impact that early-life exposure to chemotherapy has upon
542 somatosensory development. Here we have investigated
543 the effects of cisplatin treatment in young rodents and
544 upon the maturing nociceptive systems in the periphery
545 nervous system and dorsal horn of the spinal cord. Our
546 data show that early-life cisplatin treatment leads to a
547 delayed but prolonged pain hypersensitivity that is associ-
548 ated with a remodeling of the sensory nervous systems.

549 **Cisplatin induced pain in adult childhood cancer**
550 **survivors**

551 CIPN is one of the most common side-effects and can be
552 a treatment terminating ailment. The DRG sensory
553 neurons are damaged by chemotherapy and a number
554 of rodent studies have investigated this in the adult

555 whereby mitochondrial dysfunction (Flatters and
556 Bennett, 2006; Jin et al., 2008) and/or hindered growth
557 factor support (Vencappa et al., 2015) are primary causes
558 of CIPN. However, despite the extensive research in
559 humans and rodents to investigate adult CIPN, to date
560 minimal research has been undertaken to investigate
561 childhood cancers and the consequent treatment effects
562 on quality of life. Childhood cancers are rare, however
563 the 10-year survival rate for children surviving cancer is
564 75–80%. Therefore it is a clinical and moral necessity that
565 the quality of life for these cancer survivors needs to be
566 considered, especially as these pediatric patients are still
567 undergoing significant bodily development. It is reported
568 that ~50% of 10,397 adult childhood cancer survivors
569 highlight pain as a side-effect of treatment (Lu et al.,
570 2011), and many are dependent on prescribed analgesia
571 medication (Lu et al., 2011). Childhood cancer patients
572 who have undergone chemotherapy (e.g. vincristine, cis-
573 platin, methotrexate) treatment display signs of sensory
574 neuropathic pain later in life, typically associated with ado-

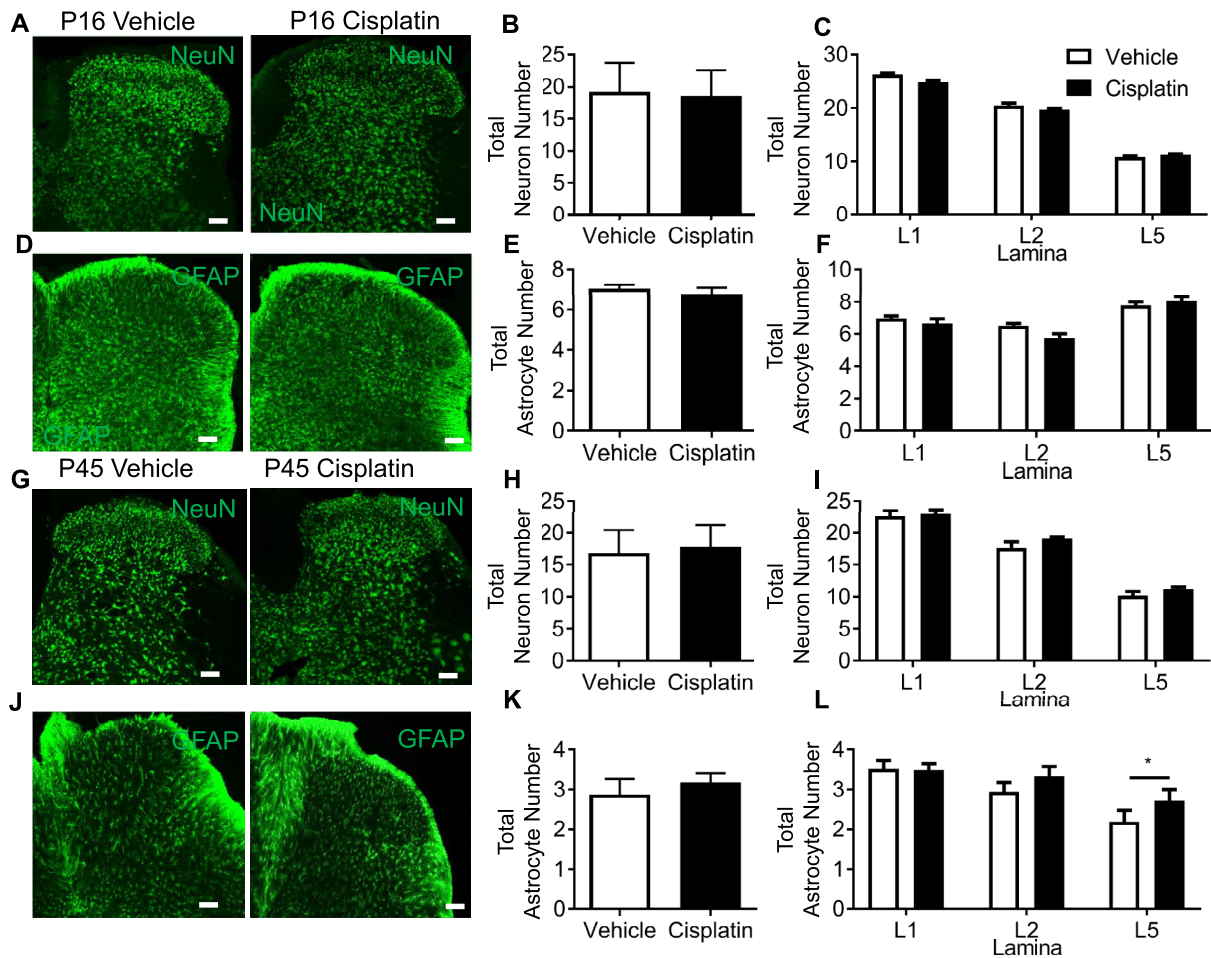


Fig. 11. Cisplatin treatment early in life does not alter sensory neuron number and increases astrocytic activation in the dorsal horn. In P16 age-matched rats that were treated with either cisplatin or vehicle demonstrate no change in [A–B] total neuron number (NeuN) in the dorsal horn. When comparing lamina there were also no differences in [C] total neuron number per laminae. [D–E] Astrocyte (GFAP) number was also unchanged in the dorsal horn in P16 age-matched rats treated with either cisplatin or vehicle. There were no differences in [F] total astrocyte number across lamina I, II and V. In adult (P45) rats treated with cisplatin early in life there were no differences in [G–I] total neuron number (NeuN) across dorsal horn laminae when compared to vehicle-treated age-matched controls. [J–K] There was no change in total astrocyte (GFAP) number, however, there was an increase in lamina V of GFAP-positive astrocytes ($P < 0.05$ Unpaired t test; vehicle = 5, cisplatin $n = 5$) (scale bar = 100 μm).

575 lence (Lu et al., 2011; Ness et al., 2013; Khan et al.,
 576 2014). Patients who are diagnosed with cancer in early
 577 life (< 10 years old) and are then assessed later in life,
 578 present symptoms of CIPN such as hypersensitivity to
 579 mechanical stimulation in the hands and arms (Gilchrist
 580 and Tanner, 2013; Gilchrist et al., 2014), as well as hall-
 581 marks of sensory neurodegeneration (Lu et al., 2011;
 582 Khan et al., 2014). These symptoms occur many years
 583 after diagnosis and the end of treatment (> 7 yrs)
 584 Phillips et al., 2015; Khan et al., 2014. The data presented
 585 in this study complement these human studies, whereby
 586 early-life treatment with cisplatin leads to the development
 587 of neuropathic pain, but this pain does not present until
 588 later in life. This delay in the manifestation of neuropathic
 589 pain until adulthood when the injury was in early life has
 590 been seen with other animal models (McKelvey et al.,
 591 2015) and recently presented following early-life exposure
 592 to vincristine (Schappacher et al., 2017). It must be noted

593 that acute toxicity and hypersensitivity from chemother-
 594 apy exposure has been demonstrated (Joseph and
 595 Levine, 2009). In this study acute pain (within hours of
 596 drug administration) were not investigated and could be
 597 missed. However, heat hypersensitivity develops at a
 598 timepoint much later following final cisplatin injections
 599 despite regular nociceptive testing. This highlights our pri-
 600 mary focus of this study on understanding alterations to
 601 the sensory nervous system in adulthood following cis-
 602 platin treatment. This further explains our rationale for
 603 our chosen methodology for the development of this child-
 604 hood model of CIPN. Cisplatin administration in humans
 605 is typically multiple cycles of treatment (Zsiros et al.,
 606 2013) and adult rodent models have been developed to
 607 explore CIPN in this setting (Mao-Ying et al., 2014). How-
 608 ever, these studies aimed to determine how cisplatin
 609 impacts upon sensory neuron development therefore
 610 requiring a focussed delivery timeline to allow identifica-

tion of any nociceptive changes. These data provide the first insight into how cancer treatment can impact upon the developing sensory nervous system and consequently chronic pain in adult childhood cancer survivors.

Cisplatin exposure is associated with long lasting pain

CIPN is long-lasting in adults with pain persisting for many months or years post termination of treatment (Flatters and Bennett, 2006; Paice, 2009; Paice, 2011). Sensory neuronal apoptosis is thought to be restricted to the peripheral nervous system (Jacobs et al., 2010), with neuropathy symptoms typically displayed in the extremities e.g. hands or feet. Targeting of which, can alleviate platinum-based chemotherapy-induced sensory neuropathy (Joseph and Levine, 2009). Despite this obvious impact upon the sensory nervous system particularly in adults and known implications of chemotherapy toxicity to children, minimal information is available on chemotherapy-induced pain in adult childhood cancer survivors. There are increased neurological symptoms in adult childhood cancer patients such as auditory complications (Grewal et al., 2010). Here we present evidence that young animals treated with cisplatin develop a delayed but long lasting pain. The sensory nervous system develops and matures over the first weeks of life; C fiber integration into the spinal dorsal horn and both intrinsic and descending inhibitory tone within the dorsal horn is established (Jennings and Fitzgerald, 1998; Koch et al., 2012), vastly improving motor and sensory acuity (Fitzgerald, 2005). In association neuropathic pain only becomes established 3 weeks postnatally if a traumatic nerve injury is introduced during the initial 2 weeks of life (Vega-Avelaira et al., 2012; McKelvey et al., 2015). Our data demonstrate that cisplatin treatment administered during the second week of life induces neuropathic pain that develops 22 days post-natally. This is highly comparable to studies in pediatric patients whereby pain is uncommon in young children (Walco et al., 2010), however neurological complications and pain are increasingly common in patients with increasing age (Phillips et al., 2015).

Understanding how such chemotherapy treatments impact upon the developing sensory nervous system allows us to design and provide suitable analgesic relief and treatment management to these patients. It is known that if you introduce a noxious insult e.g. traumatic nerve or incisional injury to young individuals that long-lasting pain does not necessarily become apparent until later in life. This has been displayed recently in rats and mice where a spared nerve injury in the first post-natal week led to a delayed hyperalgesia (McKelvey et al., 2015). In addition, this is comparable to human studies where pain does not present until much later in life (Fitzgerald, 2005; Vega-Avelaira et al., 2012; Fitzgerald and McKelvey, 2016). Furthermore, in neonatal animals there is a significant loss of sensory neurons in the initial post-natal weeks (Coggeshall et al., 1994) which is exacerbated following nerve injury (Himes and Tessler, 1989). It has been reported that cisplatin and other platinum-based drugs induce neuronal apoptosis (Gill and Windebank, 1998). However, cisplatin treatment in post-

natal week 2 does not lead to alterations in DRG neuronal number or sub-classifications in the immature (P16) tissue but demonstrates increases in neuronal stress presented by increases in cleaved caspase III when compared to the vehicle group in the immature group. Interestingly the tissue extracted from adult (P45) rats treated with cisplatin also do not display any difference in DRG number or alterations in DRG neuron soma size compared to vehicle control animals therefore cisplatin-induced sensory neuropathy is not associated with neuronal apoptosis in this instance. However, following a traumatic nerve injury, sensory DRG neurons have the capability to regenerate, hyperinnervating peripheral and central targets (Himes and Tessler, 1989; Shortland and Fitzgerald, 1994). There can be expansive remodeling of peripheral nerve innervation patterns in the skin (Reynolds and Fitzgerald, 1995) as well as into the dorsal horn of the spinal cord (Shortland and Fitzgerald, 1994); which is typified by a spike in nerve growth factor expression in neonatal and adult rodents (Lewin and Mendell, 1994; Constantinou et al., 1994). Cisplatin treatment in the second post-natal week led to striking a hyperinnervation in adults, with an increased IENF into the plantar skin of CGRP+ve and PGP9.5+ve nerve fibers. This is accompanied by alterations in the innervation pattern of the sensory afferent central terminals with elevated levels and/or alterations in depth of lamina innervation displayed by C fibers and A fibers. As mentioned sensory axonal and nerve fiber processes do have the ability to recover following chemotherapy treatment (Flatters and Bennett, 2006), however such chemotherapy treatments potentially initiates aberrant growth of sensory nerve fibers due to the impact on developing tissues as highlighted whereby NGF is administered in neonatal peripheral tissues (Lewin and Mendell, 1994; Constantinou et al., 1994). This is in contrast to earlier timepoints where IENF innervation is reduced following cisplatin treatment. It is known that the sensory nerve can regenerate following an insult (Ma et al., 2011) and that treatment or disease induces uncontrolled aberrant sensory nerve fiber growth, to which is associated with chronic pain development such as in rodent models of arthritis (Ghilardi et al., 2012) and cancer pain (Bloom et al., 2011). We postulate here that despite initial suppression of the regenerative capacity (decrease in ATF3 expression (Vencappa et al., 2015) following cisplatin exposure, endogenous regenerative mechanisms are induced driving this aberrant growth. Further understanding of these mechanisms is needed to allow us to potentially identify key mechanisms associated with chronic pain development.

Changes in C fiber innervation patterns peripherally and centrally we believe could be attributable to the delayed but long-lasting pain induced by cisplatin. Furthermore, the onset of mechanical and heat hyperalgesia can be associated with the onset of C fiber sensitization (Djouhri et al., 2001; Djouhri et al., 2006; Hulse et al., 2010; Hulse, 2016). This can be prevented through the inhibition of the NGF-TrkA axis (Djouhri et al., 2001). It is plausible that cisplatin-induced survivorship pain is mediated by TrkA-dependent mechanisms, which is widely acknowledged as a key component of

732 sensory neuron trophic support and chronic pain develop-
 733 ment (Bloom et al., 2011; Ghilardi et al., 2012). Induction
 734 of NGF-TrkA signaling is highly plausible as the percent-
 735 age of sensory DRG neurons expressing TrkA (tropomy-
 736 sin receptor kinase A) as well as dorsal horn innervation
 737 of TrkA-positive sensory afferent terminals were upregu-
 738 lated in the cisplatin adult (P45) group versus vehicle
 739 age-matched controls. Aberrant branching of sensory
 740 nociceptors has been widely associated with the develop-
 741 ment of hyperalgesia and peripheral sensory nerve sensi-
 742 tization typically associated with disease such as
 743 arthritis (Jimenez-Andrade and Mantyh, 2012) and bone
 744 cancer (Jimenez-Andrade et al., 2010; Bloom et al.,
 745 2011). With regards to A fiber function; A fiber sensi-
 746 tization has been associated with onset of chronic pain
 747 (Tsantoulas et al., 2012) and that A fiber sensitization
 748 occurs comparably in inflammatory arthritis in both hairy
 749 and glabrous skin (Drake et al., 2014). However, our con-
 750 clusions as regards delayed onset of chronic pain need to
 751 also consider that descending control can impact upon
 752 nociceptive processing with regards to A fiber inputs, to
 753 the instance that A fiber induced chronic pain can be
 754 blocked via activation of inhibitory descending modulation
 755 (Drake et al., 2014). This is in addition to decreased A
 756 fiber innervation into the hairy surface of the hindpaw
 757 which would lead to reduced sensory dexterity (Boada
 758 et al., 2010). Therefore delayed mechanical allodynia in
 759 this instance could be due to inhibitory descending control
 760 or alternatively due to lack of sensitization on the hairy
 761 side of the hindpaw.

762 CIPN is a common complaint of adults receiving
 763 chemotherapy, especially cisplatin, in addition to the
 764 inability to sleep, low mood and difficulty performing
 765 everyday tasks. It is important in clinical practice to
 766 understand the long-term effects of chemotherapy on
 767 children and the developing nervous system. Childhood
 768 cancer survivors appear to have a delayed onset of
 769 neuropathic pain compared to adults for whom there is
 770 an immediate onset of allodynia and hyperalgesia.
 771 Plasticity in the immature nervous system and impact of
 772 cisplatin treatment leads to the normal development of
 773 nociceptive pathways being disrupted. A change in pain
 774 processing due to chemotherapy treatment, manifesting
 775 as hypersensitivity, could impact patient quality of life.
 776 Few studies, however, have documented the late effects
 777 of chemotherapeutic agents in pediatric patients or the
 778 future impact of CIPN. Hence, the hyperalgesia
 779 observed here holds clinical importance with many
 780 patients experiencing late effects of their treatment.
 781 Clinically, an intervention which prevents abnormal
 782 maturation yet provides symptom relief may be viable in
 783 the future.

784 *Acknowledgments*—All authors have read and approved final
 785 version of the manuscript. RPH, GH, EM, JL were involved with
 786 the experimental design, performed the research, and analyzed
 787 data. RPH and GH wrote the manuscript with contributions from
 788 JL and final approval from all authors. We would like to acknowl-
 789 edge assistance/advice given by Prof DO Bates (School of Med-
 790 icine, University of Nottingham) and Dr LF Donaldson (School of
 791 life Sciences, University of Nottingham). This work was sup-
 792 ported by the Biotechnology and Biological Sciences Research

Council [grant number BB/I001565/1]; and by the University of
 Nottingham. There are no conflicts of interest to disclose.

793
 794

795 REFERENCES

- Bloom AP, Jimenez-Andrade JM, Taylor RN, Castaneda-Corral G,
 Kaczmarek MJ, Freeman KT, et al. (2011) Breast cancer-
 induced bone remodeling, skeletal pain, and sprouting of sensory
 nerve fibers. *J Pain* 12(6):698–711.
- Boada MD, Houle TT, Eisenach JC, Ririe DG (2010) Differing
 neurophysiologic mechanosensory input from glabrous and hairy
 skin in juvenile rats. *J Neurophysiol* 104(6):3568–3575.
- Clanton NR, Klosky JL, Li C, Jain N, Srivastava DK, Mulrooney D,
 et al. (2011) Fatigue, vitality, sleep, and neurocognitive
 functioning in adult survivors of childhood cancer: a report from
 the Childhood Cancer Survivor Study. *Cancer* 117
 (11):2559–2568.
- Coggeshall RE, Pover CM, Fitzgerald M (1994) Dorsal root ganglion
 cell death and surviving cell numbers in relation to the
 development of sensory innervation in the rat hindlimb. *Brain*
Res Dev Brain Res 82(1–2):193–212.
- Constantinou J, Reynolds ML, Woolf CJ, Safieh-Garabedian B,
 Fitzgerald M (1994) Nerve growth factor levels in developing rat
 skin: upregulation following skin wounding. *NeuroReport* 5
 (17):2281–2284.
- Djohri LDD, Robertson A, Newton R, Lawson SN (2001) Time
 course and nerve growth factor dependence of inflammation-
 induced alterations in electrophysiological membrane properties
 in nociceptive primary afferent neurons. *J Neurosci* 21
 (22):8722–8733.
- Djohri L, Koutsikou S, Fang X, McMullan S, Lawson SN (2006)
 Spontaneous pain, both neuropathic and inflammatory, is related
 to frequency of spontaneous firing in intact C-fiber nociceptors. *J*
Neurosci 26(4):1281–1292.
- Drake R, Hulse R, Lumb B, Donaldson L (2014) The degree of acute
 descending control of spinal nociception in an area of primary
 hyperalgesia is dependent on the peripheral domain of afferent
 input. *J Physiol* 592(16):3611–3624.
- Fitzgerald M (2005) The development of nociceptive circuits. *Nat Rev*
Neurosci 6(7):507–520.
- Fitzgerald M, McKelvey R (2016) Nerve injury and neuropathic pain –
 a question of age. *Exp Neurol* 275(Pt 2):296–302.
- Flatters SJ, Bennett GJ (2006) Studies of peripheral sensory nerves
 in paclitaxel-induced painful peripheral neuropathy: evidence for
 mitochondrial dysfunction. *Pain* 122(3):245–257.
- Ghilardi JR, Freeman KT, Jimenez-Andrade JM, Coughlin KA,
 Kaczmarek MJ, Castaneda-Corral G, et al. (2012)
 Neuroplasticity of sensory and sympathetic nerve fibers in a
 mouse model of a painful arthritic joint. *Arthritis Rheum* 64
 (7):2223–2232.
- Gilchrist LS, Tanner L (2013) The pediatric-modified total neuropathy
 score: a reliable and valid measure of chemotherapy-induced
 peripheral neuropathy in children with non-CNS cancers. *Support*
Care Cancer 21(3):847–856.
- Gilchrist LS, Marais L, Tanner L (2014) Comparison of two
 chemotherapy-induced peripheral neuropathy measurement
 approaches in children. *Support Care Cancer* 22(2):359–366.
- Giles PA, Trezise DJ, King AE (2007) Differential activation of protein
 kinases in the dorsal horn in vitro of normal and inflamed rats by
 group I metabotropic glutamate receptor subtypes. *Neuropharmacology*
 53(1):58–70.
- Gill JS, Windebank AJ (1998) Cisplatin-induced apoptosis in rat
 dorsal root ganglion neurons is associated with attempted entry
 into the cell cycle. *J Clin Invest* 101(12):2842–2850.
- Grewal S, Merchant T, Raymond R, McInerney M, Hodge C, Shearer
 P (2010) Auditory late effects of childhood cancer therapy: a
 report from the Children's Oncology Group. *Pediatrics* 125(4):
 e938–e950.

- 859 Himes BT, Tessler A (1989) Death of some dorsal root ganglion
860 neurons and plasticity of others following sciatic nerve section in
861 adult and neonatal rats. *J Comp Neurol* 284(2):215–230.
- 862 Hulse RP (2016) Identification of mechano-sensitive C fibre
863 sensitization and contribution to nerve injury-induced
864 mechanical hyperalgesia. *Eur J Pain* 20(4):615–625.
- 865 Hulse R, Wynick D, Donaldson L (2010) Intact cutaneous C fibre
866 afferent properties in mechanical and cold neuropathic allodynia.
867 *Eur J Pain* 14(6):565.
- 868 Hulse RP, Beazley-Long N, Ved N, Bestall SM, Riaz H, Singhal P,
869 et al. (2015) Vascular endothelial growth factor-A165b prevents
870 diabetic neuropathic pain and sensory neuronal degeneration.
871 *Clin Sci* 129(8):741–756.
- 872 Jacobs S, McCully CL, Murphy RF, Bacher J, Balis FM, Fox E (2010)
873 Extracellular fluid concentrations of cisplatin, carboplatin, and
874 oxaliplatin in brain, muscle, and blood measured using
875 microdialysis in nonhuman primates. *Cancer Chemother
876 Pharmacol* 65(5):817–824.
- 877 Jennings E, Fitzgerald M (1998) Postnatal changes in responses of
878 rat dorsal horn cells to afferent stimulation: a fibre-induced
879 sensitization. *J Physiol* 509(Pt 3):859–868.
- 880 Jimenez-Andrade JM, Mantyh PW (2012) Sensory and sympathetic
881 nerve fibers undergo sprouting and neuroma formation in the
882 painful arthritic joint of geriatric mice. *Arthritis Res Ther* 14(3):
883 R101.
- 884 Jimenez-Andrade JM, Bloom AP, Stake JI, Mantyh WG, Taylor RN,
885 Freeman KT, et al. (2010) Pathological sprouting of adult
886 nociceptors in chronic prostate cancer-induced bone pain. *J
887 Neurosci* 30(44):14649–14656.
- 888 Jin HW, Flatters SJ, Xiao WH, Mulhern HL, Bennett GJ (2008)
889 Prevention of paclitaxel-evoked painful peripheral neuropathy by
890 acetyl-L-carnitine: effects on axonal mitochondria, sensory nerve
891 fiber terminal arbors, and cutaneous Langerhans cells. *Exp
892 Neurol* 210(1):229–237.
- 893 Joseph E, Levine J (2009) Comparison of oxaliplatin- and cisplatin-
894 induced painful peripheral neuropathy in the rat. *J Pain* 10
895 (5):534–541.
- 896 Khan R, Hudson M, Ledet D, Morris E, Pui C, Howard S, et al. (2014)
897 Neurologic morbidity and quality of life in survivors of childhood
898 acute lymphoblastic leukemia: a prospective cross-sectional
899 study. *J Cancer Surviv* 8(4):688–696.
- 900 Koch SC, Tochiki KK, Hirschberg S, Fitzgerald M (2012) C-fiber
901 activity-dependent maturation of glycinergic inhibition in the spinal
902 dorsal horn of the postnatal rat. *PNAS* 109(30):12201–12206.
- 903 Kunin-Batson AS, Lu X, Balsamo L, Graber K, Devidas M, Hunger
904 SP, et al. (2016) Prevalence and predictors of anxiety and
905 depression after completion of chemotherapy for childhood acute
906 lymphoblastic leukemia: a prospective longitudinal study. *Cancer
907* 122(10):1608–1617.
- 908 Lewin GR, Mendell LM (1994) Regulation of cutaneous C-fiber heat
909 nociceptors by nerve growth factor in the developing rat. *J
910 Neurophysiol* 71(3):941–949.
- 911 Lorenzo L-E, Ramien M, St Louis M, De Koninck Y, Ribeiro-Da-Silva
912 A (2008) Postnatal changes in the rexed lamination and markers
913 of nociceptive afferents in the superficial dorsal horn of the rat. *J
914 Comp Neurol* 509:604.
- 915 Lu Q, Krull KR, Leisenring W, Owen JE, Kawashima T, Tsao JC,
916 et al. (2011) Pain in long-term adult survivors of childhood cancers
917 and their siblings: a report from the Childhood Cancer Survivor
918 Study. *Pain* 152(11):2616–2624.
- 919 Ma CH, Omura T, Cobos EJ, Latremoliere A, Ghasemlou N, Brenner
920 GJ, et al. (2011) Accelerating axonal growth promotes motor
921 recovery after peripheral nerve injury in mice. *J Clin Invest* 121
922 (11):4332–4347.
- 923 Mao-Ying QL, Kavelaars A, Krukowski K, Huo XJ, Zhou W, Price TJ,
924 et al. (2014) The anti-diabetic drug metformin protects against
925 chemotherapy-induced peripheral neuropathy in a mouse model.
926 *PLoS ONE* 9(6):e100701.
- 927 McKelvey R, Berta T, Old E, Ji R, Fitzgerald M (2015) Neuropathic
928 pain is constitutively suppressed in early life by anti-inflammatory
929 neuroimmune regulation. *J Neurosci* 35(2):457–466.
- McWhinney SR, Goldberg RM, McLeod HL (2009) Platinum 930
neurotoxicity pharmacogenetics. *Mol Cancer Ther* 8(1):10–16. 931
- Ness K, Jones K, Smith W, Spunt S, Wilson C, Armstrong G, et al. 932
(2013) Chemotherapy-related neuropathic symptoms and 933
functional impairment in adult survivors of extracranial solid 934
tumors of childhood: results from the St. Jude Lifetime Cohort 935
Study. *Arch Phys Med Rehabil* 94(8):1451–1457. 936
- Paice J (2009) Clinical challenges: chemotherapy-induced peripheral 937
neuropathy. *Semin Oncol Nurs* 25(2): S8-19. 938
- Paice JA (2011) Chronic treatment-related pain in cancer survivors. 939
Pain 152(3 Suppl): S84-9. 940
- Park H, Stokes J, Pirie E, Skahen J, Shterman Y, Yaksh T (2013) 941
Persistent hyperalgesia in the cisplatin-treated mouse as defined 942
by threshold measures, the conditioned place preference 943
paradigm, and changes in dorsal root ganglia activated 944
transcription factor 3: the effects of gabapentin, ketorolac, and 945
etanercept. *Anesth Analg* 116(1):224–231. 946
- Park SB, Goldstein D, Krishnan AV, Lin CS, Friedlander ML, Cassidy 947
J, et al. (2013) Chemotherapy-induced peripheral neurotoxicity: a 948
critical analysis. *CA Cancer J Clin* 63(6):419–437. 949
- Phillips SM, Padgett LS, Leisenring WM, Stratton KK, Bishop K, Krull 950
KR, et al. (2015) Survivors of childhood cancer in the united 951
states: prevalence and burden of morbidity. *Cancer Epidemiol* 952
Biomark Prev 24(4):653–663. 953
- Reynolds ML, Fitzgerald M (1995) Long-term sensory 954
hyperinnervation following neonatal skin wounds. *J Comp* 955
Neurol 358(4):487–498. 956
- Schappacher KA, Styczynski L, Baccei ML (2017) Early life 957
vincristine exposure evokes mechanical pain hypersensitivity in 958
the developing rat. *Pain* 158(9):1647–1655. 959
- Seretny M, Currie GL, Sena ES, Ramnarine S, Grant R, MacLeod 960
MR, et al. (2014) Incidence, prevalence, and predictors of 961
chemotherapy-induced peripheral neuropathy: a systematic 962
review and meta-analysis. *Pain* 155(12):2461–2470. 963
- Shortland P, Fitzgerald M (1994) Neonatal sciatic nerve section 964
results in a rearrangement of the central terminals of saphenous 965
and axotomized sciatic nerve afferents in the dorsal horn of the 966
spinal cord of the adult rat. *Eur J Neurosci* 6(1):75–86. 967
- Smith MA, Seibel NL, Altekruze SF, Ries LA, Melbert DL, O'Leary M, 968
et al. (2010) Outcomes for children and adolescents with cancer: 969
challenges for the twenty-first century. *J Clin Oncol* 28
970 (15):2625–2634. 971
- Ta LE, Espeset L, Podratz J, Windebank AJ (2006) Neurotoxicity of 972
oxaliplatin and cisplatin for dorsal root ganglion neurons 973
correlates with platinum-DNA binding. *Neurotoxicology* 27
974 (6):992–1002. 975
- Thakur M, Rahman W, Hobbs C, Dickenson AH, Bennett DL (2012) 976
Characterisation of a peripheral neuropathic component of the rat 977
monoiodoacetate model of osteoarthritis. *PLoS ONE* 7(3):
978 e33730. 979
- Tsantoulas C, Zhu L, Shaifta Y, Grist J, Ward JP, Raouf R, et al. 980
(2012) Sensory neuron downregulation of the Kv9.1 potassium 981
channel subunit mediates neuropathic pain following nerve injury. 982
J Neurosci 32(48):17502–17513. 983
- Uhelski ML, Khasabova IA, Simone DA (2015) Inhibition of 984
anandamide hydrolysis attenuates nociceptor sensitization in a 985
murine model of chemotherapy-induced peripheral neuropathy. *J* 986
Neurophysiol 113(5):1501–1510. 987
- van As JW, van den Berg H, van Dalen EC (2012) Medical 988
interventions for the prevention of platinum-induced hearing loss 989
in children with cancer. *Cochrane Database Syst Rev* 5:1.
990 CD009219. 991
- Vega-Avelaira D, McKelvey R, Hathway G, Fitzgerald M (2012) The 992
emergence of adolescent onset pain hypersensitivity following 993
neonatal nerve injury. *Mol Pain* 8(30). 994
- Vencappa S, Donaldson LF, Hulse RP (2015) Cisplatin induced 995
sensory neuropathy is prevented by vascular endothelial growth 996
factor-A. *Am J Transl Res* 7(6):1032–1044. 997
- Walco GA, Dworkin RH, Krane EJ, LeBel AA, Treede RD (2010) 998
Neuropathic pain in children: special considerations. *Mayo Clin* 999
Proc 85(3 Suppl):S33–S41. 1000

1001	Ward E, DeSantis C, Robbins A, Kohler B, Jemal A (2014) Childhood	and surgery: final results of the SIOPEL-3HR study. J Clin Oncol	1007
1002	and adolescent cancer statistics, 2014. CA Cancer J Clin 64	28(15):2584–2590.	1008
1003	(2):83–103.	Zsiros J, Brugieres L, Brock P, Roebuck D, Maibach R, Zimmermann	1009
1004	Zsiros J, Maibach R, Shafford E, Brugieres L, Brock P, Czauderna P,	A, et al. (2013) Dose-dense cisplatin-based chemotherapy and	1010
1005	et al. (2010) Successful treatment of childhood high-risk	surgery for children with high-risk hepatoblastoma (SIOPEL-4): a	1011
1006	hepatoblastoma with dose-intensive multiagent chemotherapy	prospective, single-arm, feasibility study. Lancet Oncol 14	1012
		(9):834–842.	1013

1014
1015
1016

(Received 15 June 2017, Accepted 16 November 2017)
(Available online xxxx)

UNCORRECTED PROOF